The International Journal of **Medical Robotics** and **Computer Assisted Surgery**

THE INTERNATIONAL JOURNAL OF MEDICAL ROBOTICS AND COMPUTER ASSISTED SURGERY
Int J Med Robotics Comput Assist Surg 2013; **9**: 109–118.
Published online 18 September 2012 in Wiley Online Library (wileyonlinelibrary.com) **DOI:** 10.1002/rcs.1459

ORIGINAL ARTICLE

Preliminary study of a novel method for conveying corrected image volumes in surgical navigation

Amber L. Simpson[1]*
Prashanth Dumpuri[2]
Janet E. Ondrake[1]
Jared A. Weis[3]
William R. Jarnagin[4]
Michael I. Miga[1]

[1]*Department of Biomedical Engineering, Vanderbilt University, Nashville, TN, USA*

[2]*Pathfinder Therapeutics Inc., Nashville, TN, USA*

[3]*Vanderbilt University Institute of Imaging Science, Nashville, TN, USA*

[4]*Department of Surgery, Memorial Sloan Kettering Cancer Center, New York, NY, USA*

*Correspondence to: A. L. Simpson, VU Station B 351631, Nashville, TN 37235, USA.
E-mail: amber.l.simpson@vanderbilt.edu

Accepted: 21 August 2012

Abstract

Background Commercial image-guided surgery systems rely on the fundamental assumption that preoperative medical images represent the physical state of the patient in the operating room. The guidance display typically consists of a three-dimensional (3D) model derived from medical images and three orthogonal views of the imaging data. A challenging question in image-guided surgery is: what happens when the images used in the guidance display no longer correspond to the current geometric state of the anatomy and guidance information is still desirable?

Methods We modify the conventional display with two techniques for incorporating a displacement field from a finite-element model into the guidance display and present a preliminary study of the effect of our method on performance with a simple surgical task. The topic of this paper is methods for conveying the computational model solution, not the model itself. To address the integration of the computational model solution into the display, a novel method of applying the deformation to the tool tip was developed, which quickly corrects for deformation but also maintains the pristine nature of the preoperative images. We compare the proposed technique to an existing method that applies the deformation field to the image volume.

Results A pilot study compared mean performance with our method of applying the deformation to the tool tip and the conventional technique. These methods were statistically similar with respect to accuracy of localization ($p < 0.05$) and amount of time ($p < 0.05$) required for localization of the target.

Conclusions These results suggest that our new technique can be used in place of the computationally expensive task of deforming the image volume, without affecting the time or accuracy of the surgical task. Most notably, our work addresses the problem of incorporating deformation correction into the guidance display and offers a first step toward understanding its effect on surgical performance. Copyright © 2012 John Wiley & Sons, Ltd.

Keywords image-guided surgery; surgical navigation displays; finite element models; deformation correction; user study

Introduction

In the traditional image-guided surgery paradigm, imaging of the patient occurs preoperatively. A patient-specific three-dimensional (3D) model is constructed by isolating structures of interest from surrounding tissues in the imaging data, and this model is used by the surgeon in the operating room for guiding the placement of surgical tools after it is brought into correspondence

with the physical state of the patient. In a typical surgical guidance display, the surgeon is presented with orthogonal views of the preoperative medical image volume, a view of the 3D surface model and renderings of the surgical tools with respect to the anatomy. This approach is appropriate for bony structures that do not deform from their preoperative state. However in soft tissue surgery, deformation occurs due to manipulation of the organ, application of pharmaceuticals and gravity, such that the surgeon's guidance display can often no longer correspond to the physical reality of the patient.

In the case of the liver, systemic studies have shown that the liver can non-rigidly deform by up to 2 cm, which compromises the accuracy of systems that rely on assumptions of organ rigidity (1). In open abdominal liver tumour removal surgeries, significant deformation occurs when the liver is detached from the supporting ligamenture for inspection of the organ. Prior to the hepatectomy, the liver is packed with surgical sponges and mobilized for better access to the tumour area, which results in further deformation (2).

Intraoperative magnetic resonance imaging (MRI) and computed tomography (CT) methods have been proposed by many authors for the solution to the organ-shift problem (1,3). Typically, a high-resolution data-rich image volume is acquired prior to surgery and one or more lower-resolution images are attained during surgery. Correspondence is established from the intraoperative state of the anatomy to the preoperative state, so that surgical plans and other imaging datasets [e.g. from functional MRI, diffusion tensor imaging, positron emission tomography (PET), to name a few] obtained preoperatively can be utilized. The mechanism of deformation correction, in this case, is the non-rigid registration algorithm. Another method of compensating for deformation is to use a low-cost intraoperative data acquisition device such as intraoperative ultrasound (4–6) or laser-range scanning technology (7–10) coupled with sophisticated computational models. In this model-updated paradigm, intraoperative data is matched to preoperative data, and deformation is accounted for using a finite-element model of the target anatomy under deformation. There is a need to update the guidance display with any of these deformation schemes. In the case of intraoperative imaging, one could simply update the display with the intraoperative image if the resolution of the image were sufficient.

In this study, a novel method of incorporating deformation correction is introduced and its efficacy is compared to that of the more traditional design, whereby computed deformations are applied directly to the preoperative image volume. Intraoperatively deforming the image volume requires > 1.5 min to complete. Our new method requires virtually no time, since the deformation update is only computed for the current location of the tool, rather than for the entire image volume. We compare surgical performance with these techniques in a user study employing data from image-guided liver interventions. The criteria for comparison are the time it takes to navigate to a subsurface target and the accuracy with which this task is achieved.

Deformation correction framework

The deformation correction framework used in this study requires many distinctive steps, which are illustrated in Figure 1 and briefly described in this section. In this paper, one specific aspect of deformation correction using mathematical models is investigated, and that is the update of the guidance display with the computed deformation field (the final box in the chart). A detailed description of this deformation correction scheme can be found in related work (2). In summary, the framework consists of the following:

Preoperative phase

1. *CT scan*. A CT scan of the target anatomy is obtained, the same as in conventional liver surgery.
2. *Segmentation and model construction*. The liver is segmented from neighbouring structures using a semi-automatic method (11) and a 3D surface model is constructed using marching cubes (12).
3. *Mesh generation*. The 3D surface model is smoothed and parameterized using FastRBF toolkit (FarField Technology, Christchurch, New Zealand). Using the 3D surface model, a volumetric tetrahedral mesh is generated for use with our finite element methodology (13).

Intraoperative phase

1. *Surface data acquisition*. A 3D surface representation of the deformed liver is acquired using a laser range

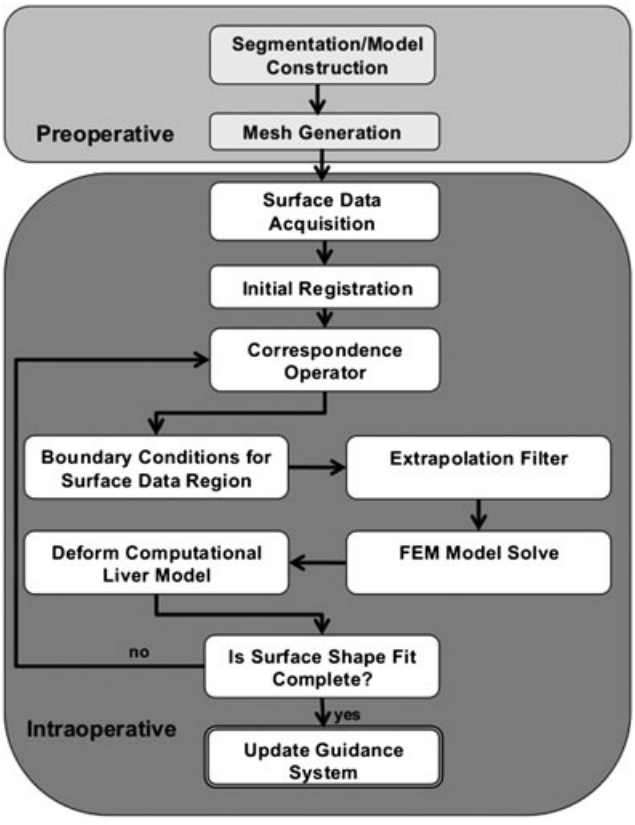

Figure 1. Typical workflow for the deformation correction framework. This paper addresses updating the guidance system, depicted in the last box of the diagram

DOI: 10.1002/rcs

scanner (LRS; Pathfinder Therapeutics Inc., Nashville, TN, USA). The scanner collects 3D surface data (as a point cloud) and a two-dimensional (2D) texture of the scanned object.
2. *Registration*. The LRS surface is registered to the preoperative 3D model using landmarks/features identified on the preoperative model and corresponding landmarks/features designated in surgery with an optically-tracked stylus (the falciform ligament, round ligament and inferior ridges are used for this purpose). Initial alignments are achieved with the iterative closest-point algorithm (ICP) (14) and refined using a variant of ICP, which weights salient features from the liver more than the remainder of the LRS surface (15).
3. *Correspondence determination*. The residual closest-point distances between the preoperative and intraoperative organ surfaces are computed to assist in further alignment.
4. *Boundary condition generation and model update*. After establishing an initial alignment and correspondence between the preoperative and intraoperative surfaces using rigid registration and correspondence operator, respectively, the alignment is then improved by accounting for the non-rigid deformation using a computational model. One strategy could be to apply the residual displacements computed in the correspondence step as boundary conditions for the computational model; however, the LRS data are typically incomplete and only exists for areas of the organ in direct line of sight with the device. As a result, the volumetric deformations provided are often only useful in a very local area that may or may not include the entire surgical focus. In this study we used sparse extrapolative techniques that attempt to predict a distribution of correspondence outside the focal LRS region, using a surface Laplacian (2,16). Once a complete boundary condition set is known, the computational model can be run and a volumetric prediction of organ deformation is generated.
5. *Guidance display update*. Once a deformation field is computed, the guidance display requires updating with the information. In this paper, two methods towards the incorporation of non-rigid deformation fields have been implemented and compared: the application of the deformation field from the computational model to (a) the image volume and (b) the tip of the surgeon's tool.

Time is a key factor in the clinical realization of our framework. The time required in the intraoperative phase of the framework is of particular importance, since this is the amount of time that the surgical staff will be waiting for an update of the guidance display. Our software implementation of the intraoperative phase was developed with full parallelization in mind, using PETSc and MPICH2 (Argonne National Laboratories, USA). All computations were performed on a parallel cluster of eight 2.4 GHz dual-core AMD Opteron processors. For a single typical case (a clinical case used in this study), salient feature registration required 31 s, correspondence determination 9 s and model update 44 s, for a total of 84 s. The image deformation phase required an additional 99 s. Removing the necessity of deforming the image cuts the time required intraoperatively from 183 to 90 s, or roughly in half.

Related work

Miga *et al*. (10,17,24) proposed a method of updating preoperative image volumes with intraoperative updates provided by finite-element models. Once the model update was performed, calculating the displacement for each voxel using the finite-element basis functions deformed the preoperative images. The voxel intensities were assigned based on backcasting the model to the undeformed state. Miga *et al*. (17,24) demonstrated a complete image update, including deformation due to organ sag, retraction, partial resection and complete resection. Ferrant *et al*. (18) employed a similar approach, by interpolating from each element in the mesh to the image grid and applying their modelling technique to tissue resection. Vigneron *et al*. (19) also explored similar methods by removing the tumour from the deformed images by simply assigning the background colour to the tumour location. In the final deformed image volume, the resected tissue was absent from the display. Zhuang *et al*. (20) reported an image deformation method identical to that of Miga *et al*. and a modelling pipeline as described in the previous section, but further validated the techniques using intraoperative MRI.

These methods address the development of modelling techniques as well as quantitative aspects of deformation correction, but only tangentially address the problem of integrating deformation into operating room (OR) workflow and, specifically, the systemic investigation of the effect of displaying deformed preoperative images on surgical efficacy. In this paper, we provide two distinct contributions. First, we describe a new method of conveying deformation to the surgeon, by applying the correction to the tip of the surgeon's tool rather than to the image volume. Second, we compare the proposed technique with the image volume deformation technique and study the effect of these schemes on surgical performance. To our knowledge, this is the first experiment of its kind whereby surgical navigation is directly tested within the context of using deformation-corrected image-guided display techniques.

Materials and methods

In this section, we describe the source of the patient data used as stimuli for each task in this navigation study, the methods used to integrate the calculated deformation field into the guidance display, and the design of the navigation study. It is important to note that the computational details and accuracy assessment of the biomechanical model have been described in other work [see e.g. Dumpuri *et al*. (2)]; we are simply using the data and models for

DOI: 10.1002/rcs

computing the guidance environment stimuli employed in the user study.

Hepatectomy data source

The datasets for three patients undergoing partial hepatectomy were selected from a 75 patient clinical trial of image-guided liver surgery conducted by our industrial partner, Pathfinder Therapeutics Inc. (Nashville, TN, USA), and our academic partners, Memorial Sloan Kettering Cancer Center, Pittsburgh Medical Center, and the University of Florida, Gainsville Medical Center. All data were obtained with written patient consent and under the auspices of the institutional review boards of the respective institutions. For the navigation study described herein, we used the data acquired preoperatively and intraoperatively in the clinical trial and applied our biomechanical models retrospectively, using the methods outlined in the previous section and illustrated in Figure 1.

Guidance display updating methods

In the study, subjects were presented with a guidance display with either a) corrected preoperative images or b) our new method in which the deformation field is applied to the tool tip.

Deformation field applied to preoperative image volumes
We applied the volumetric deformation field to the preoperative images to generate a deformed image volume for use in navigation tasks. Due to the nature of the framework depicted in Figure 1, the liver is the only object for which a volumetric deformation field is calculated; therefore, the position and orientation of the other, non-liver, objects within the deformed CT image volume remain unchanged, as compared to the rigidly registered undeformed CT image volume. To create a deformed image volume, initially the voxels within the liver extents are assigned the background intensity. Using the mesh (step 3 of the preoperative phase, above) and the calculated deformation field resulting from intraoperative data acquisition (steps 1–4 in the intraoperative phase), a deformed mesh is generated. Once complete, all the voxels within the deformed elements are identified and the linear tetrahedral basis functions can be used to interpolate the appropriate reverse deformation field. Once the reverse displacement for each voxel in the deformed geometry is known, it can be used to determine the appropriate intensity for each voxel, using a trilinear interpolation of the eight nearest neighbour voxels in the original undeformed reference image volume.

Two sample image volumes before and after deformation correction are shown in Figure 2. The first image volume (Figure 2a, b) has moderate deformation, while the deformation in the second volume (Figure 2c, d) is more severe. Note that the background anatomy is simply overlaid on the deformed liver domain and therefore does not take into account any deformation. The bright white spot represents the simulated tumour.

Deformation field applied to instrument tip
Our novel method of introducing deformation into the guidance display is to apply the appropriate displacement value from the volumetric deformation field to the tip of the surgical tool, while leaving the preoperative images intact. In a traditional guidance system framework, a global rigid transformation is applied to the position and orientation of the surgical instrument, so that the instruments are superimposed on image volumes. With our method, the global rigid registration transformation is applied, followed by a local non-rigid refinement of the transformed tool tip.

The rigid registration transforms the surgical instruments from physical space in the operating room to the preoperative image space. The non-rigid refinement step corrects the position of the tool on the images, using the volumetric deformation field computed by the finite-element model. Since the volumetric deformation field does not exist for every voxel in the preoperative image volume (i.e. deformation is only computed at the nodes of the finite element mesh and can only be interpolated internally), an interpolation (if the transformed tool position is within the extents of the liver) or an extrapolation (if the transformed tool position lies outside of the extent of the liver) is required. Similar to image deforming, the finite element basis functions can be used to estimate the displacement vectors at any point within the domain of the organ.

For applying the non-rigid correction outside of the liver, an envelope around the organ is defined whereby the nearest displacement on the liver mesh is assigned to the voxel envelope but with a linearly decreasing magnitude as a function of the distance to the mesh. The equation that expresses this weighting scheme, $\mathbf{D}_i$, is:

$$\mathbf{D}_i = (-0.1\ \ d_i + 1)\,\mathbf{V} \text{ for } |d_i| \leq 10 \text{ mm (for all } i \text{ in } voxels_{env}) \quad (1)$$

where d_i is the unsigned closest-point distance to the surface of the volume mesh in millimeters, $\mathbf{V}$ is the respective non-rigid displacement vector associated with that position in the computational model and $voxels_{env}$ are the voxels inside of the envelope.

The effect of equation 1 is that as a tracked stylus approaches the physical organ, a smooth non-rigid adjustment to the stylus (based on the equation 1 extrapolation) is performed until the user touches the organ where model-based interpolations exist. If the extrapolative envelope did not exist, the surgeon might experience a flickering effect if the stylus lost any contact with the organ surface while swabbing/interrogating for surgery, because the areas outside of the organ would be undefined. We should also note that the voxels outside the extrapolative envelope have no added correction and are subject only to the initial rigid alignment.

An example rendering of the magnitude of the displacements including the envelope is illustrated in Figure 3.

DOI: 10.1002/rcs

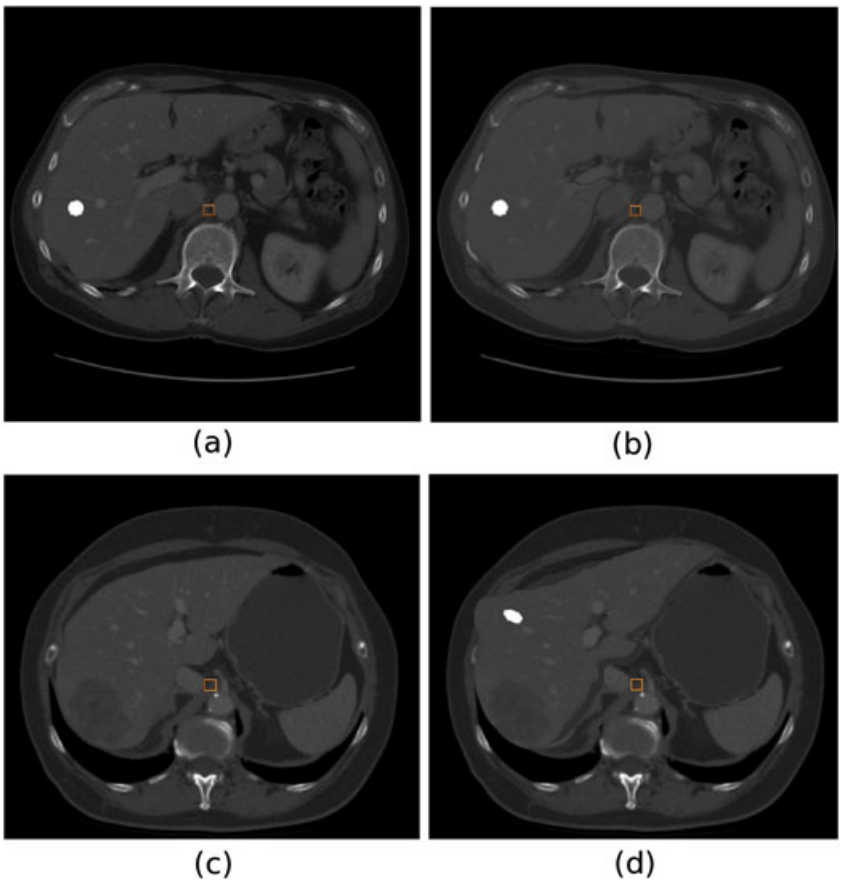

Figure 2. Axial slices from the CT image volume before and after deformation correction for two sets of patient data: a patient dataset in which the applied deformation was relatively small, a CT slice (a) before and (b) after deformation correction; and a second patient dataset in which the applied deformation was relatively large, a CT slice (c) before and (d) after correction. The bright white spot is the tumour. In (c), the deformation is large enough to move the tumour to a different slice in the volume. The square represents the current location of the tool

Dark blue indicates no displacement; lighter blue represents the envelope surrounding the organ. The envelope serves to gradually increase the magnitude of the displacements from the outside of the organ (where there is no displacement) to the inside of the organ (where there is displacement). Without the envelope, the tool could move in a disjointed manner when moving from the inside of the organ to the outside.

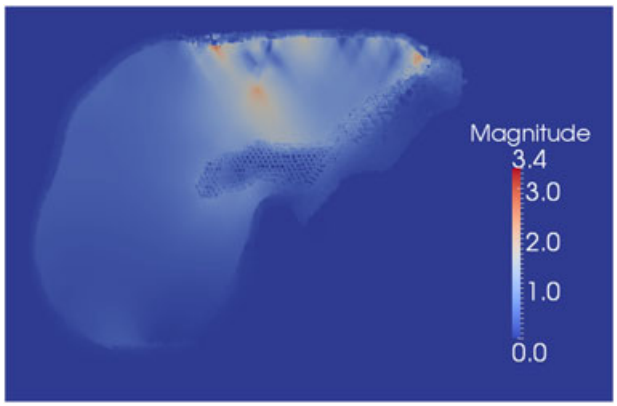

Figure 3. An example of the magnitude of displacements that are applied to the instrument tip in our method. Dark blue indicates zero displacement, which surrounds the organ. The envelope is shown in lighter blue. The largest magnitudes are rendered in red

A comparison of a surgical guidance display with no correction, correction applied by deforming the images and correction applied to the tip of the tool is depicted in Figure 4. The same patient dataset is used with the surgical tool positioned on the (bright white) tumour target for all figures. In Figure 4a no correction is applied; hence, the cross-hairs are not centred on the tumour. In Figure 4b, c, correction is applied and the cross-hairs are centred on the tumour. The navigation study used only conditions (b) and (c); the uncorrected volume is shown for comparison only. A fourth view in the guidance display (not depicted in the figure), consisting of the 3D model with a rendering surgical instrument, was also displayed.

User study

This study mimics the localization of small tumours in image-guided liver surgery. In this task, the surgeon must find a subsurface target (tumour). We quantify the success of this task by measuring the time it takes to complete the task and the accuracy of the position of the tool on the virtual display, as recorded by the optical tracking system.

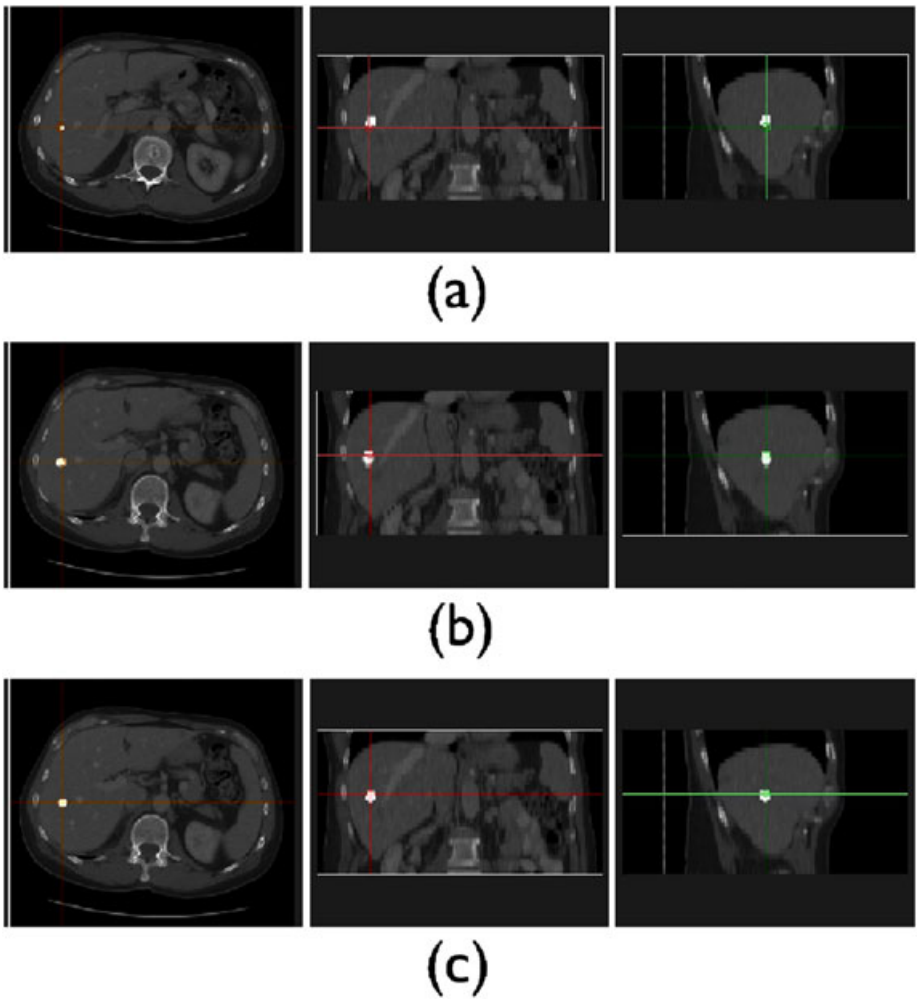

Figure 4. Axial, coronal and sagittal views from the surgical navigation system using: (a) no correction; (b) correction applied to the deformed image; and (c) correction applied to the tool tip. The cross-hairs represent the current location of the tool. The surgical instrument was fixated such that these images were captured with respect to the same physical location. The bright white spot is the tumour

Hypothesis

Localization and speed are better if the computed deformations are applied to the tip of the tool rather than by deforming the preoperative image volume.

Subjects

Eleven subjects performed the experiment. Two senior residents from Vanderbilt University Medical Center, our affiliated research hospital, both with experience with commercial surgical systems, participated in the study. Nine subjects from the university community with no experience in surgical navigation also completed the study.

Apparatus

A Polaris Spectra optical tracking system (Northern Digital Inc., Waterloo, ON, Canada) tracked the position and orientation of a passive target attached to the apparatus and the surgical stylus. Eight metal targets, each 6.5 mm in diameter, were mounted to an optical bench in an irregular arrangement. Modelling clay obscured the targets from view. An 18 inch computer monitor placed in the line of sight of the subject (approximately 1 m in front) displayed guidance information to the subject during the experiment (see Figure 5).

Stimuli

We placed two virtual tumours (spheres with diameter 6.5 mm) in each of the three hepatectomy patient datasets, for a total of six virtual tumours for use in the study. The virtual tumour was rendered in bright white in the CT volume within the orthogonal views, and as a 3D model in the model view of the guidance display. The array of targets in the apparatus were aligned with the virtual tumours by touching the physical targets with the calibrated optically tracked stylus and registering this with the known position of the tumour in the volume. When the subject touched the physical target, the virtual tool in the guidance display touched the virtual tumour.

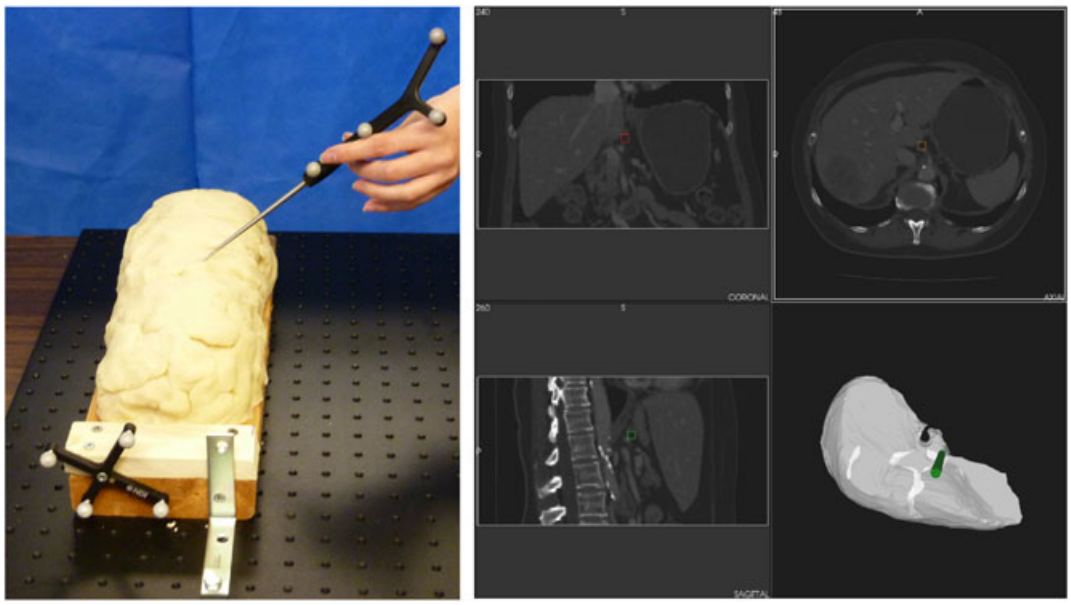

Figure 5. The apparatus (left) and the navigation system (right) used in our study. A Polaris Spectra optical tracking system (not pictured) tracked the position and orientation of the tool and apparatus (patient). Modelling clay obscured the metal targets (tumours)

The size of the physical targets corresponded to the size of the simulated tumours in the CT.

Subjects were presented with the guidance display. Their task was to use the display to navigate to the physical tumour obscured by modelling clay.

Experiment

Each subject was trained using two preliminary trials in order to reduce the effects of learning. Each subject was presented with six trials with the deformed image volume (see Figure 4b) and six trials with the deformed tip (see Figure 4c). Within each group of six, the order in which tasks were presented to subjects was randomized. To further address the effects of learning and fatigue, half of the subjects performed trials with the deformed image volume prior to trials with the deformed tip.

The results of the study were analysed using hypothesis testing wherein a null hypothesis states no effect (or no difference) between groups and the alternative hypothesis indicates the presence of an effect or a difference in groups. A research hypothesis typically predicts an effect or difference; generally a researcher expects the alternative hypothesis to be supported (21).

Equivalence testing is a recent development in statistical methodology used for testing proof of similarity between groups within a small amount, Δ; measures that differ by at most Δ are considered to be equivalent (22). Δ is chosen according to the application. In the equivalence testing in this study, $\Delta = 2$ mm was chosen as a clinically meaningful difference in accuracy due to inaccuracies in optical tracking and instrument calibration. $\Delta = 60$ s was chosen as a clinically meaningful time differential in performing a guidance task. We chose this value because, in the USA, operating room time is billed by the minute.

Results

We measured the accuracy with which subjects localized the virtual target with the tool and the time required to place the tool. Mean localization error and time for trials in which the image volume was deformed was 4.7 ± 2.1 mm and 73 ± 57 s, respectively. Mean localization error and time for trials in which the tool tip was deformed was 3.7 ± 1.6 mm and 77 ± 65 s. These results are summarized in Table 1.

A one-way analysis of variance (ANOVA) tested for significant differences in performance (accuracy and time) across all conditions. The test found significant differences in accuracy ($F = 10.850$, $p < 0.001$) but not time ($F = 0.085$, $p = 0.771$). The results for mean accuracy and time by condition for each trial are plotted in Figure 6 and for each subject in Figure 7.

A two-sided t-test tested for similarity in performance (accuracy and time required for localizing structures of interest in the task) across all conditions. The test indicated that the theoretical difference is within a clinically unimportant interval for accuracy ($\Delta = 2$ mm, $p \leq 0.05$) and time ($\Delta = 60$ s, $p \leq 0.05$).

We also tested whether the magnitude of the deformation had any effect on performance. We did this by measuring the 3D distance between each tumour in the deformed and undeformed states. A one-way ANOVA tested for

Table 1. Accuracy and time results for both conditions

	Accuracy (mm)				Time (s)			
Condition	Mean	SD	Min	Max	Mean	SD	Min	Max
Deformed volume	4.7	2.1	0.5	9.2	73	57	10	273
Deformed tool	3.7	1.6	0.7	7.9	77	65	13	373
Total	4.2	1.9	0.5	9.2	75	60	10	373

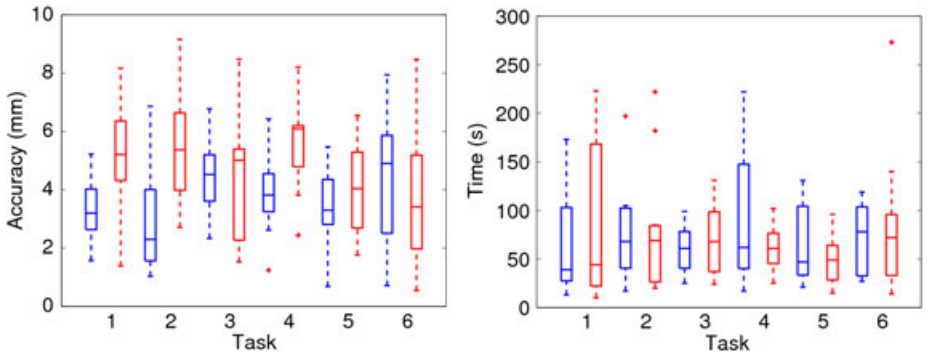

Figure 6. The effect of navigation method on mean accuracy (left) and time (right) for the deformed tip (blue) and deformed image volume (red) trials, plotted by task. Subjects performed better with deformation applied to the tool tip ($p < 0.001$)

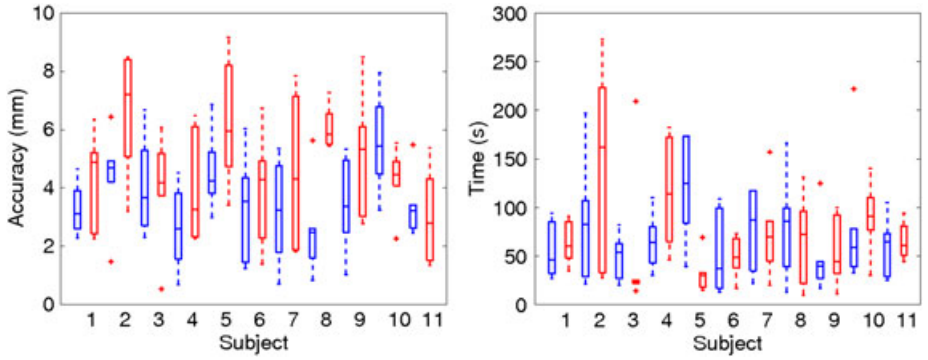

Figure 7. The effect of navigation method on mean accuracy (left) and time (right) for the deformed tip (blue) and the deformed image volume (red) trials plotted by subject. Subjects performed better with deformation applied to the tool tip ($p < 0.001$)

significant differences in performance (accuracy and time) with respect to the magnitude of deformation. The test found no significant differences in accuracy ($F = 0.666$, $p = 0.650$) or time ($F = 0.737$, $p = 0.597$).

Discussion

We studied two simple methods of updating a surgical navigation system with a deformation field computed using a biomechanical finite-element model. Our proposed method of applying the deformation to the tip of the surgical tool requires virtually no computational overhead, since the deformation is only computed for the current location of the tool rather than for the entire image volume. For the datasets in this study, the process of deforming the image volume required > 1.5 min to complete on an eight processor 3.2 GHz Intel i7 CPU with 12 GB of RAM. Removing this step is important because after an update has been computed in the operating room the surgeon must wait for the result before resuming surgery. Time expense is one of the fundamental challenges of using computational models in surgery.

We were very encouraged that our new method of applying the deformations to the tip of the surgeon's tool resulted in a statistically significant improvement in the localization accuracy over conducting the same test with its image-deformed counterpart for guidance ($p < 0.001$). The difference in means between the deformed image volume trials and the deformed tip trials is on the order of 1 mm (see Table 1) with the deformation of the tool tip performing better. Indeed, equivalence testing demonstrated that the accuracy of both methods were statistically similar to within 2 mm. Our argument is not one of accuracy improvement; we simply show that our method is just as good (in terms of surgical performance) as the established method of conveying a computational model solution. The premise is that, since our method requires no computational overhead and has no negative performance repercussions, it may be a better methodological direction for the incorporation of non-rigid changes to guidance displays.

One might expect that our new method could potentially reduce localization accuracy, since small movements in physical space could translate to non-linear scale movements in the virtual display, resulting in a target-chasing effect. For example, moving from large to small displacements could cause the tool to 'jump' on the display. In practice, since we are applying smoothed boundary deformation onto a homogeneous material, the linear elastic constitutive equations used in the mechanical model would dictate that the displacements should be smooth, without discontinuities or large jumps. If the mesh were too coarse, accurately capturing the smooth displacement distribution would be problematic, but since there is a sufficient level of mesh refinement in the model, the displacement field should be smooth. This was supported

in our results. Specifically, we tested the effect of the magnitude of the deformation on performance and found no significant differences.

With respect to time for task completion, equivalence testing results indicated that the two approaches are indistinguishable from each other and that any difference is of no practical consequence. The primary advantage of applying the deformation to the tool tip, rather than to the image volume, is that the preoperative image volume(s) remains pristine, i.e. the high resolution preoperative diagnostic scan as well as any additional data that has been registered to that scan (e.g. functional MRI, PET scans, etc.). By demonstrating that our technique does not affect surgical performance, the stylus can be instantly rendered on every tomographic image set simultaneously.

At this time, we chose not to test the effect of navigation without deformation correction. With the same apparatus, we could have simply shown subjects a third condition in which the undeformed volume is shown with no means of correction. If we give subjects imperfect intraoperative information, we are no longer studying the effect of navigation methods but rather the effect of performing with poor data. It would be relatively straightforward to set up a study in which surgeons always perform better with the corrected displays; this would have more to do with the accuracy of the deformation correction scheme rather than the navigation method, which is what we were concerned with in this study. Here, we chose to isolate the effect of the type of deformation correction display on performance. Nevertheless, these preliminary results are exciting and speak to new studies in spatial cognition that have not been attempted within the deformation correction community.

As another note of interest, the two experts who took part in our study correspond to subjects 4 and 5 in Figure 7. While we do not have enough expert subjects for a statistical comparison based on experience, it is interesting to note their performance in Figure 7. With respect to accuracy, both experts found that the deformation correction applied to the tip produced more accurate localization than the guidance based on the deformed image; however, with respect to the time to execute, the results were mixed, with one favouring the transformed tip and the other favouring the deformed image. While these observations are anecdotal, they do provide a glimpse into some fascinating questions remaining that are concerned with surgical cognition within the context of image guidance.

The primary criticism of our study is that we chose non-expert subjects for participation. The purpose of this study was to show that, within a very specific guidance task, performance (time and accuracy) could be affected by navigation method. This study is a preliminary study; further investigation with surgeons in the operating theatre is needed before final conclusions can be drawn. However, we needed to first show the potential of the method. A prospective study is under way in collaboration with our neurosurgical colleagues at Vanderbilt University Medical Center. In this investigation, the surgeon is presented with three conditions in succession, a guidance display with: (a) no correction; (b) deformation correction by deformed images; and (c) deformation correction by deformed tool tip. The surgeon's task is to interrogate the surface and (when possible) subsurface extents of the brain and resection cavity with the tracked surgical tools and to report which display best represents physical reality better.

Not many studies have been devoted to an assessment of how surgical performance is affected by the visualization methods adopted for CT and MR images; as such this area deserves further investigation. The lack of studies could be because it is challenging to define a task representative of a typical use of a guidance display that can be statistically analysed. In addition, an in-depth study of such factors would require extensive clinical integration and collaboration, with the potential of increasing OR time.

Finally, we believe that this study addresses a new paradigm in surgical navigation. Galloway and Peters posit that: 'one of the fundamental concepts of [image-guided surgery], which is that images represent the present state of the physiology, is only the first approximation' (23). Indeed, increased processing power and memory mean that sophisticated mathematical models can be solved within the OR environment. A crucial step in this development is the integration of these models into surgical displays.

Conclusion

We have presented an approach for updating the guidance display with deformation fields calculated from finite-element models. In a preliminary study of surgical task performance, using our novel method of applying the deformation to the tip of the tool rather than the traditional method of applying deformation to the image volume, accuracy was shown to be statistically equivalent to within 2 mm ($p < 0.05$), while the time to navigate was shown to be equivalent ($p < 0.05$). When one considers the wealth of preoperative data available, application of the model correction to the tool tip approach is an enabling technique for efficient decision making within the changing intraoperative environment.

Acknowledgements

This work is funded by the National Institutes of Health, partly under the National Cancer Institute (Grant No. R01CA162477) and partly under the National Institute for Neurological Disorders and Stroke (Grant No. R01NS049251); the former was involved with data collection, processing of abdominal images and the creation of the method of applying the deformation to the tip of the surgeon's tool, the latter with image-deforming strategies for model-corrected guidance. We disclose that Dr Miga is a co-founder and holds equity in Pathfinder Therapeutics Inc., Nashville, TN, USA.

Conflict of interest

The authors have stated explicitly that there are no conflicts of interest in connection with this article.

Funding

No specific funding.

References

1. Heizmann O, Zidowitz S, Bourquain H, *et al*. Assessment of intraoperative liver deformation during hepatic resection: prospective clinical study. *World J Surg* 2010; **34**(8): 1887–1893.
2. Dumpuri P, Clements LW, Dawant BM, *et al*. Model-updated image-guided liver surgery: preliminary results using surface characterization. *Prog Biophys Mol Biol* 2010; **103**(2–3): 197–207.
3. Martin RC. Intraoperative magnetic resonance imaging ablation of hepatic tumors. *Am J Surg* 2005; **189**(4): 388–394.
4. Beller S, Hunerbein M, Lange T, *et al*. Image-guided surgery of liver metastases by three-dimensional ultrasound-based optoelectronic navigation. *Br J Surg* 2007; **94**(7): 866–875.
5. Chopra SS, Hunerbein M, Eulenstein S, *et al*. Development and validation of a three-dimensional ultrasound-based navigation system for tumor resection. *Eur J Surg Oncol* 2008; **34**(4): 456–461.
6. Lunn KE, Paulsen KD, Roberts DW, *et al*. Displacement estimation with co-registered ultrasound for image guided neurosurgery: a quantitative *in vivo* porcine study. *IEEE Trans Med Imaging* 2003; **22**(11): 1358–1368.
7. Audette MA, Siddiqi K, Ferrie FP, *et al*. An integrated range-sensing, segmentation and registration framework for the characterization of intrasurgical brain deformations in image-guided surgery. *Comput Vis Image Und* 2003; **89**: 226–251.
8. Cash DM, Miga MI, Sinha TK, *et al*. Compensating for intraoperative soft-tissue deformations using incomplete surface data and finite elements. *IEEE Trans Med Imaging* 2005; **24**(11): 1479–1491.
9. Cash DM, Miga MI, Glasgow SC, *et al*. Concepts and preliminary data toward the realization of image-guided liver surgery. *J Gastrointest Surg* 2007; **11**(7): 844–859.
10. Miga MI, Paulsen KD, Lemery JM, *et al*. Model-updated image guidance: initial clinical experience with gravity-induced brain deformation. *IEEE Trans Med Imaging* 1999; **18**(10): 866–874.
11. Hermoye L, Laamari-Azjal I, Cao Z, Annet L, Lerut J, Dawant BM, Van Beers BE. Liver segmentation in living liver transplant donors: comparison of semiautomatic and manual methods. *Radiology* 2005; **234**(1): 171–178.
12. Lorensen WE, Cline HE. Marching cubes: a high resolution 3D surface construction algorithm. *SIGGRAPH Comput Graph* 1987; **21**(4): 163–169.
13. Sullivan JM, Charron G, Paulsen KD. A three-dimensional mesh generator for arbitrary multiple material domains. *Finite Elem Anal Design* 1997; **25**(3–4): 219–241.
14. Besl PJ, McKay ND. A method for registration of 3D Shapes. *IEEE T Pattern Anal* 1992; **14**(2): 239–255.
15. Clements LW, Chapman WC, Dawant BM, *et al*. Robust surface registration using salient anatomical features for image-guided liver surgery: algorithm and validation. *Med Phys* 2008; **35**(6): 2528–2540.
16. Miga MI, Dumpuri P, Simpson AL, *et al*. The sparse data extrapolation problem: strategies for soft-tissue correction for image-guided liver surgery. In *SPIE Medical Imaging 2011: Visualization, Image-Guided Procedures, and Modeling Conference; Lake Buena Vista, FL, USA*, Wong KH, Holmes DR (eds.) eds. SPIE, 2011.
17. Miga MI, Roberts DW, Kennedy FE, *et al*. Modeling of retraction and resection for intraoperative updating of images during surgery. *Neurosurgery* 2001; **49**(1): 75–84 discussion, 84–85..
18. Ferrant M, Nabavi A, Macq B, *et al*. Serial registration of intraoperative MR images of the brain. *Med Image Anal* 2002; **6**(4): 337–359.
19. Vigneron LM, Warfield SK, Robe PA, *et al*. 3D XFEM-based modeling of retraction for preoperative image update. *Comput Aided Surg* 2011; **16**(3): 121–134.
20. Zhuang DX, Liu YX, Wu JS, *et al*. A sparse intraoperative data-driven biomechanical model to compensate for brain shift during neuronavigation. *Am J Neuroradiol* 2011; **32**(2): 395–402.
21. Sheskin DJ. *Handbook of Parametric and Nonparametric Tests*. Chapman & Hall: Boca Raton, FL, 2004.
22. Tryon WW. Evaluating statistical difference, equivalence, and indeterminacy using inferential confidence intervals: an integrated alternative method of conducting null hypothesis statistical tests. *Psychol Methods* 2001; **6**(4): 371–386.
23. Galloway R, Peters T. Overview and history of image-guided interventions. In *Image-guided Interventions: Technology and Applications*, Peters T, Cleary K (eds.) eds. Springer: New York, 2008; 1–21.
24. Miga MI, Paulsen KD, Hoopes PJ, *et al*. *In vivo* quantification of a homogeneous brain deformation model for updating preoperative images during surgery. *IEEE Trans Biomed Eng* 2000; **47**(2): 266–273.

DOI: 10.1002/rcs